

Integration of Star and Inertial Sensors for Spacecraft Attitude Determination

Kedong Wang¹, Tongqian Zhu¹, Yujie Qin¹, Chao Zhang¹ and Yong Li²

¹(School of Astronautics, Beihang University, Beijing 100191, China)

²(School of Civil and Environmental Engineering, University of New South Wales, Sydney, NSW 2052, Australia)

(E-mail: wangkd@buaa.edu.cn)

A new integration of the acquisition and tracking modes is proposed for the integration of a Celestial Navigation System (CNS) and a Strapdown Inertial Navigation System (SINS). After the integration converges in the acquisition mode, it switches to the tracking mode. In the tracking mode, star pattern recognition is unnecessary and the integration is implemented in a cascaded filter scheme. A pre-filter is designed for each identified star and the output of the pre-filter is fused with the attitude of the SINS in the cascaded navigation filter. Both the pre-filter and the navigation filter are designed in detail. The measurements of the pre-filter are the positions on the image plane of one identified star. Both the starlight direction and its error are estimated in the pre-filter. The estimated starlight directions of all identified stars are the measurements of the navigation filter. The simulation results show that both the reliability and accuracy of the integration are improved and the integration is effective when only one star is identified in a period.

KEY WORDS

1. Star sensor.
2. Celestial navigation system.
3. Inertial navigation system.
4. Kalman filter.

Submitted: 8 September 2016. Accepted: 30 April 2017. First published online: 27 June 2017.

1. INTRODUCTION. The Strapdown Inertial Navigation System (SINS), composed of gyroscopes and accelerometers, is totally autonomous. It can provide position, velocity, and attitude of the host vehicles at the frequency of 100 Hz or higher, but its errors accumulate with running time so that it cannot maintain high accuracy for a long time (Bar-Itzhach et al., 1982). Hence, it is necessary to integrate the SINS with other navigation systems, such as the Celestial Navigation System (CNS) composed of a star sensor, to compensate for the SINS accumulated errors (Xu and Fang, 2008; Rad et al., 2014; Ning et al., 2016). The CNS is also autonomous and can determine the vehicle's attitude with the accuracy of one arc-second or higher in the inertial frame (i-frame) (Liebe, 2002; Percival et al., 2008; Silani and Lovera, 2006). Its error does not accumulate with running time. It is popular to use a large Field-Of-View (FOV) star sensor in a CNS (Liebe, 1995; Ju and Junkins,

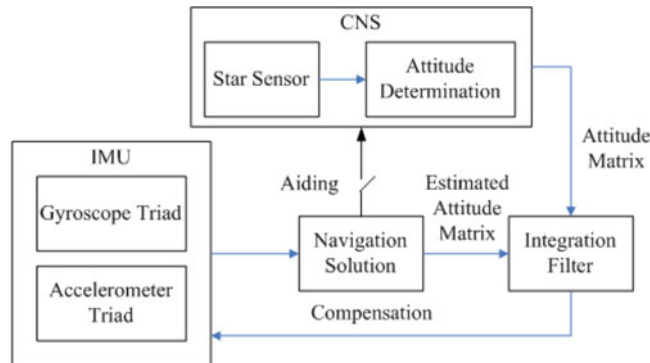


Figure 1. The existing integration of SINS/CNS.

2003). The image output by the star sensor is matched by the triangle algorithm or others to identify two or more imaged stars in all the sky to determine the vehicle's attitude (Ho, 2012; Scholl, 1995). The CNS output can be used to correct the inertial attitude error directly (Hablani, 2009). It is more popular to compensate for the SINS attitude by the CNS/SINS integration with the measurements of the attitude difference between the CNS and the SINS as shown in Figure 1 (Johnson and Phillips, 2001; Levine et al., 1990; Wu and Wang, 2011; He et al., 2014). It should be noted that the aiding from the SINS is blocked in the integration.

However, there are the following problems in the existing CNS/SINS integration where the CNS works independently.

- (i) The reliability of the CNS output needs to be improved further. If both the starlight direction and its error can be estimated, the Attitude Determination (AD) accuracy can be improved by excluding the stars with larger errors of starlight direction (Batista et al., 2011; Wang et al., 2014). However, the errors of starlight direction are usually not provided in the CNS output. The potential risk of the integration with the measurements of the CNS attitude is that the stars with low accuracy may reduce the integration accuracy.
- (ii) The availability of the CNS output is low. Star pattern recognition in all the sky is not only time consuming but also easy to mismatch so that the matching success rate is not high, in particular when the Signal-to-Noise Ratio (SNR) value of the image is low. Although the matching success rate can be improved when the star sensor works in the tracking mode, the matching process is still prone to failure during fast manoeuvres of the host vehicle. The integration will not be updated if the image matching fails. Moreover, at least two stars must be identified to determine the vehicle attitude if an angular separation algorithm is employed to match the image with the star catalogue. Three or more stars must be identified if the triangle algorithm or similar is used (Ho, 2012). That is, if one or two stars are identified, their information will be discarded and the integration will not be updated.

To resolve these problems, a new CNS/SINS integration is proposed. There are two modes, acquisition and tracking, in the integration. The acquisition mode is shown in Figure 1 but the SINS aiding is switched on. The tracking mode is illustrated in Figure 2. A similar

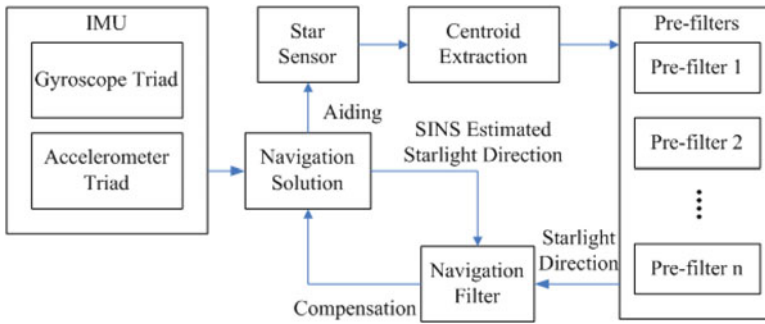


Figure 2. Tracking mode of the proposed integration of SINS/CNS.

integration has been proposed for other systems, such as the tightly-coupled integration of SINS with a Global Positioning System (GPS) receiver (Lashley et al., 2009).

When the CNS is initialised or restarted after losing stars, the integration works in the acquisition mode. In this mode, the CNS works independently and the star image is matched with the star catalogue for a regional sky which is determined by the SINS output. The star image is also compensated for and restored with the aid of the SINS if it is smeared due to the host vehicle's manoeuvring (Wang et al., 2014). Two or more stars are identified to determine the vehicle attitude if the matching is successful. The CNS attitude is fused with the SINS output in the integration filter whose output is used to compensate for the SINS accumulated attitude error.

After a successful acquisition, the integration switches to the tracking mode. In this mode, each identified star is tracked with the aid of the SINS output so that the star image does not have to be matched even if only one star in the image can be tracked. The tracked stars in the image are not used to determine the vehicle attitude directly, but their positions are input to pre-filters to estimate their starlight directions. The cascaded navigation filter fuses the estimated starlight direction output from the pre-filter for each tracked star with the SINS attitude. The result is used to compensate for the SINS accumulated attitude error.

Sun et al. (2014) proposed a similar integration, but the star pattern recognition is indispensable and all the identified stars are assumed to have the same accuracy. Moreover, three or more identified stars are required for AD. Compared with the integration of Sun et al. (2014), our proposal has the following advantages: (i) the starlight directions and their errors are estimated by the pre-filters so that the weights of the stars in the navigation filter are assigned with regard to their estimation errors, and: (ii) the identified star can be integrated with the SINS effectively even when only one star is identified.

The rest of the paper is organised as follows. The structure of the integration is detailed in Section 2. The pre-filter for each star is designed in Section 3. The navigation filter is designed in Section 4 to fuse the starlight directions output by the pre-filters with the SINS attitude. The integration is demonstrated by simulations in Section 5. Conclusions are given in Section 6.

2. STRUCTURE OF THE INTEGRATION. Figures 1 and 2 depict the detail of the integration. In the acquisition, the star centroids are extracted from the star image first. Then, the star image is matched with the star catalogue by pattern recognition in a regional

sky with the aid of the SINS. If the SINS attitude is accurate enough, the matching success rate can be improved with a significant reduction of searching time. If two or more stars are identified by the pattern recognition, the star sensor's attitude can be determined. Since the star sensor is mounted on the vehicle in the strapdown mode, the vehicle's attitude can then be deduced after the star sensor's attitude is determined. At the same time, the SINS can also determine the vehicle's attitude independently. The vehicle's attitudes determined by both the CNS and the SINS are fused in a Kalman filter to compensate for the SINS accumulated attitude error. The vehicle's manoeuvring should be sufficiently slow to avoid the star image smearing, otherwise the star centroids are difficult to extract accurately. Hence, if the vehicle angular rate is small, e.g. less than $0.1^\circ/\text{s}$, and there are at least two identified stars, the integration can be switched to the tracking mode after several filtering epochs (e.g. 3~5 epochs) in the acquisition.

In the tracking mode, the SINS is compensated by the CNS and the CNS is aided by the SINS. What is different from the deep integration in the literature (Wu and Wang, 2011; He et al., 2014) is that the CNS is aided by the SINS before the star Centroid Extraction (CE). The smeared trace is compensated with the aid of the SINS and the compensated star image is restored by the Wiener filter first if the star image is smeared (Wang et al., 2014). The SNR value of the compensated and restored star image is improved significantly so that the star centroids can be extracted accurately. Thus, even though the vehicle is manoeuvring quickly, CE can be accomplished successfully.

After CE is fulfilled, a pre-filter is designed for each identified star to estimate its starlight direction. The measurements of the pre-filter are the star positions in the image plane. Since the pre-filters of all the identified stars work independently, they can be processed in parallel to save time. Both the starlight direction and its error can be estimated by the pre-filter. In the succeeding navigation filter, the measurements are the estimated starlight directions and the measurement noise covariance matrix is determined by the estimated errors of the starlight directions. The contribution of the starlight direction is adaptively adjusted according to its estimated error in the navigation filter. Hence, in the tracking mode, even if only one star is identified, its extracted position in the image plane can still be used to estimate the vehicle attitude.

Pattern recognition in a regional sky with the SINS aid in the acquisition mode can be found in the works of Wu and Wang (2011) and Liu et al. (2011). The tracking mode, in particular, the design of the pre-filter and the navigation filter, will be covered in the succeeding sections.

3. PRE-FILTER. The pre-filter is designed for each identified star as shown in Figure 2. The input of each pre-filter includes the positions of the corresponding identified star in the image plane and the SINS output. The pre-filter outputs the estimated starlight direction and its error covariance matrix which are the input of the succeeding navigation filter. The design of the pre-filter is detailed in this section.

3.1. State equations. For an identified star, the unit vector of its starlight direction in the star sensor frame (s-frame) is the state of its pre-filter. Assume the vector $\mathbf{X}_{\text{pre}} = [i^s \ j^s \ k^s]^T$ where i^s , j^s , and k^s are the components on the axes of the s-frame. If the Direction Cosine Matrix (DCM) from the inertial frame (i-frame) to the s-frame is \mathbf{C}_i^s , there is,

$$[i^s \ j^s \ k^s]^T = \mathbf{C}_i^s [i^i \ j^i \ k^i]^T \quad (1)$$

where $i^i, j^i,$ and k^i are the components of the vector on the axes of the i -frame. Since the starlight direction in the i -frame is invariant with time, the derivative of Equation (1) with respect to time is,

$$\frac{d}{dt} [i^s \quad j^s \quad k^s]^T = \dot{\mathbf{C}}_i^s [i^i \quad j^i \quad k^i]^T \tag{2}$$

There is,

$$\dot{\mathbf{C}}_i^s = \mathbf{\Omega}_{si}^s \mathbf{C}_i^s \tag{3}$$

where $\mathbf{\Omega}_{si}^s$ is the skew symmetric matrix of the angular rate in the s -frame $\boldsymbol{\omega}_{si}^s = [\omega_{si,x}^s \quad \omega_{si,y}^s \quad \omega_{si,z}^s]^T$. The angular rate $\boldsymbol{\omega}_{si}^s$ can be measured by the gyroscope of the SINS. If the gyroscope error is taken into account, there is,

$$\boldsymbol{\omega}_{si}^s = \tilde{\boldsymbol{\omega}}_{si}^s + \Delta\boldsymbol{\omega}_{si}^s \tag{4}$$

where $\tilde{\boldsymbol{\omega}}_{si}^s$ is the angular rate output by the gyroscope triad and $\Delta\boldsymbol{\omega}_{si}^s$ is the gyroscope error.

Substituting Equations (3) and (4) into Equation (2) yields

$$\dot{\mathbf{x}}_{pre} = \tilde{\mathbf{\Omega}}_{si}^s \mathbf{x}_{pre} - \mathbf{G} \Delta\boldsymbol{\omega}_{si}^s \tag{5}$$

where \mathbf{G} is the skew symmetric matrix of the vector $[i^s \quad j^s \quad k^s]^T$. $-\mathbf{G} \Delta\boldsymbol{\omega}_{si}^s$ can be treated as the state noise. Equation (5) is the state equation of the pre-filter for an identified star.

3.2. *Measurement equations.* The measurements of the pre-filter are the positions of the star image in the image plane, i.e., $\mathbf{z}_{pre} = [z_x \quad z_y]^T$. According to the geometry of the optical imaging of the star sensor, there is,

$$\mathbf{z}_{pre} = \begin{bmatrix} \frac{f}{k^s} & 0 & 0 \\ 0 & \frac{f}{k^s} & 0 \end{bmatrix} \begin{bmatrix} i^s \\ j^s \\ k^s \end{bmatrix} + \mathbf{v}_{pre} = \mathbf{H}_{pre} \mathbf{x}_{pre} + \mathbf{v}_{pre} \tag{6}$$

where f is the focal of the star sensor and \mathbf{v}_{pre} the measurement noise. Equation (6) is the measurement equation of the pre-filter.

The measurement noise is mainly determined by the CE error. It is assumed that the CE error of a star image at the time k is estimated as $\Delta\hat{\mathbf{z}}_{pre,k} = [\Delta\hat{z}_{x,k} \quad \Delta\hat{z}_{y,k}]^T$ and its covariance matrix is $\Delta\hat{\mathbf{R}}_{pre,k}$. If the value of \mathbf{x}_{pre} before the measurement updating at the time k , $\hat{\mathbf{x}}_{pre,k}(-)$, has been estimated, the estimated residual of the measurement is $\delta\mathbf{z}_{pre,k} = \mathbf{z}_{pre,k} - \mathbf{H}_{pre,k} \hat{\mathbf{x}}_{pre,k}(-)$. The mean of the estimated residuals for all the identified stars is written as $\delta\bar{\mathbf{z}}_{pre,k}$. The covariance matrix of $\mathbf{v}_{pre,k}$ at the time k $\mathbf{R}_{pre,k}$ is determined as,

$$\mathbf{R}_{pre,k} = \begin{cases} \Delta\hat{\mathbf{R}}_{pre,k}, & |\delta\mathbf{z}_{pre,k}| \leq |\delta\bar{\mathbf{z}}_{pre,k}| \\ \frac{|\delta\mathbf{z}_{pre,k}|^2}{|\delta\bar{\mathbf{z}}_{pre,k}|^2} \Delta\hat{\mathbf{R}}_{pre,k}, & |\delta\mathbf{z}_{pre,k}| > |\delta\bar{\mathbf{z}}_{pre,k}| \end{cases} \tag{7}$$

At the first epoch, $\mathbf{R}_{pre,1} = \Delta\hat{\mathbf{R}}_{pre,1}$. In Equation (7), the stars with the larger estimated residuals of the measurements are allocated the larger values of $\mathbf{R}_{pre,k}$, which means that the stars have the lower CE accuracy. The enlarged $\mathbf{R}_{pre,k}$ will make the covariance matrix of the estimated state error after the measurement updating $\mathbf{P}_{pre,k}(+)$ increase. When the

pre-filter converges, the steady $\mathbf{P}_{\text{pre},k}(+)$ is the covariance matrix of the measurement noise in the navigation filter for the star. That is, the star with the larger CE error will be allocated with the lower weight in the navigation filter, and vice versa.

Since the state and the measurement equations of the pre-filters are linear, the standard Kalman filter is used for the pre-filters.

3.3. *Solution to the stars moving out of the FOV.* Due to the vehicle’s manoeuvring, one star may move out of the star sensor’s FOV in a filtering epoch. One solution is to reset its pre-filter if the star image is near to or out of the border of the image plane. If a new star is identified in the current FOV, the pre-filter is allocated to it. However, this solution is effective only when the vehicle is manoeuvring slowly. In contrast, if the vehicle is manoeuvring quickly, the pre-filter will reset too frequently to be valid since the duration of a star in the FOV is too short.

An alternative solution is to reuse the pre-filter but the measurement is switched to the new identified star in the current FOV, which includes the following steps.

(i) At the time k star 1 moves out of the FOV although it is in the FOV at the time $k - 1$. Its starlight direction in the s-frame at the time k is $\mathbf{I}_{1,k}^s$. With the aid of the SINS, star 2 at time k is identified in the FOV. Its starlight direction is $\mathbf{I}_{2,k}^s$, which can be obtained by rotating $\mathbf{I}_{1,k}^s$ around the axis of $\mathbf{m} = \mathbf{I}_{1,k}^s \times \mathbf{I}_{2,k}^s$ by the angle $\theta = \arccos(\mathbf{I}_{1,k}^s \cdot \mathbf{I}_{2,k}^s)$. If the quaternion of the rotation is defined as $\mathbf{q} = \cos(\theta/2) + \mathbf{m} \sin(\theta/2) = [q_0 \ q_1 \ q_2 \ q_3]^T$, the rotation matrix is,

$$\mathbf{M} = \begin{bmatrix} q_1^2 + q_0^2 - q_3^2 - q_2^2 & 2(q_1q_2 - q_0q_3) & 2(q_1q_3 + q_0q_2) \\ 2(q_1q_2 + q_0q_3) & q_2^2 - q_3^2 + q_0^2 - q_1^2 & 2(q_2q_3 - q_0q_1) \\ 2(q_1q_3 - q_0q_1) & 2(q_2q_3 + q_0q_1) & q_3^2 - q_2^2 - q_1^2 + q_0^2 \end{bmatrix} \tag{8}$$

There is,

$$\mathbf{I}_{2,k}^s = \mathbf{M}\mathbf{I}_{1,k}^s \tag{9}$$

(ii) If the state estimation for star 1 before the measurement updating at time k $\hat{\mathbf{x}}_{\text{pre},1,k}(-)$ and its covariance matrix $\mathbf{P}_{\text{pre},1,k}(-)$ are obtained, the state estimation for star 2 before the measurement updating and its covariance matrices are,

$$\begin{cases} \hat{\mathbf{x}}_{\text{pre},2,k}(-) = \mathbf{M}\hat{\mathbf{x}}_{\text{pre},1,k}(-) \\ \mathbf{P}_{\text{pre},2,k}(-) = \mathbf{M}\mathbf{P}_{\text{pre},1,k}(-)\mathbf{M}^T \end{cases} \tag{10}$$

(iii) The measurement Equation (6) is adjusted for star 2. The extracted centroid position of star 2 in the image plane is the measurement at the time k $\mathbf{z}_{\text{pre},k}$ and $\mathbf{R}_{\text{pre},k}$ is renewed accordingly.

With the completion of the above processing, the state and the measurement equations for star 1 are switched to star 2. In this way, the pre-filters do not need to reset and can be updated continuously so that they keep working even though the vehicle is manoeuvring quickly.

4. NAVIGATION FILTER. The estimated states and the error covariance matrices of all the pre-filters are fed into the navigation filter to estimate the vehicle attitude after the pre-filters converge. Similar to the design of the pre-filters, the state and the measurement

equations are also the focus of the design of the navigation filter. Since the attitude is decoupled from the position and the velocity in the inertial frame, the vehicle position and its velocity are not included in the states of the navigation filter. The coloured noises of gyroscopes are included in the states, which are modelled as a first order Markov process for simplification of the procedure. If their models are not of a first order Markov process, the corresponding states should be modified accordingly.

4.1. *State equations.* The state equations are composed of the error equations of the strapdown attitude mechanism and the gyroscopes, which are given in the equations below (Ali and Fang, 2006). The SINS attitude error equations are written in the inertial frame at launching point (li-frame).

$$\begin{cases} \dot{\mathbf{x}} = \mathbf{F}\mathbf{x} + \mathbf{w} \\ \mathbf{x} = [\boldsymbol{\varphi}^T \quad \boldsymbol{\varepsilon}^T]^T \\ \mathbf{F} = \begin{bmatrix} \mathbf{F}_1 & \mathbf{0}_{3 \times 3} \\ \mathbf{0}_{3 \times 3} & \mathbf{F}_2 \end{bmatrix} \\ \mathbf{w} = [\mathbf{0}_{1 \times 3} \quad \mathbf{w}^T]^T \end{cases} \quad (11)$$

where $\boldsymbol{\varphi} = [\phi_x \quad \phi_y \quad \phi_z]^T$, $\boldsymbol{\varepsilon} = [\varepsilon_x \quad \varepsilon_y \quad \varepsilon_z]^T$, $\mathbf{w} = [w_x \quad w_y \quad w_z]^T$; ϕ_x , ϕ_y and ϕ_z are the vehicle attitude errors in the three directions; ε_x , ε_y and ε_z are the gyroscope errors in the b-frame; \mathbf{w} are the noises of the first order Markov process; and w_j ($j = x, y, z$) is a zero-mean Gaussian white noise. The matrices \mathbf{F}_i ($i = 1 \sim 2$) are

$$\mathbf{F}_1 = \mathbf{C}_b^{li} \quad (12)$$

$$\mathbf{F}_2 = \text{diag} \left(\left[-1/\tau_{\text{gyro}} \quad -1/\tau_{\text{gyro}} \quad -1/\tau_{\text{gyro}} \right]^T \right) \quad (13)$$

where \mathbf{C}_b^{li} is the DCM from the b-frame to the li-frame; $\text{diag}(\cdot)$ means the diagonal matrix of a vector and τ_{gyro} is the time constant of the gyroscopes.

Equation (11) is linear and time-varying since the matrix \mathbf{F} is time-varying.

4.2. *Measurement equations.* The measurements of the navigation filter are the difference between the unit vectors of the identified starlight directions estimated by the pre-filters and the SINS, which are derived as follows.

For star 1 at the time k , there is

$$\mathbf{I}_{\text{CNS},1,k}^s = \mathbf{C}_b^s \mathbf{C}_{li}^b \mathbf{I}_{1,k}^{li} \quad (14)$$

where $\mathbf{I}_{\text{CNS},1,k}^s$ is the unit vector in the s-frame without errors, $\mathbf{I}_{1,k}^{li}$ is the unit vector of the starlight direction in the li-frame acquired from the star catalogue and \mathbf{C}_b^s and \mathbf{C}_{li}^b are the DCMs from the b-frame to the s-frame and from the li-frame to the b-frame, respectively. As long as the star sensor is mounted on a vehicle, \mathbf{C}_b^s is constant and can be calibrated accurately. Therefore, it is assumed as known in the following. However, there is an error in the estimation of $\mathbf{I}_{\text{CNS},1,k}^s$ output by the pre-filter. Hence, Equation (14) can be modified as,

$$\hat{\mathbf{I}}_{\text{CNS},1,k}^s = \mathbf{C}_b^s \mathbf{C}_{li}^b \mathbf{I}_{1,k}^{li} + \mathbf{v}_{\text{CNS},1,k} \quad (15)$$

where $\mathbf{v}_{\text{CNS},1,k}$ is the starlight direction error estimated by the pre-filter.

Equation (14) can also be written as

$$\hat{\mathbf{I}}_{\text{INS},1,k}^{\text{s}} = \mathbf{C}_b^{\text{s}} \hat{\mathbf{C}}_{\text{li}}^{\text{b}} \mathbf{I}_{1,k}^{\text{li}} \tag{16}$$

where $\hat{\mathbf{I}}_{\text{INS},1,k}^{\text{s}}$ is the unit vector estimated by the SINS and $\hat{\mathbf{C}}_{\text{li}}^{\text{s}}$ is the DCM from the li-frame to the b-frame estimated by the SINS. Since there is an error in the attitude determined by the SINS, $\hat{\mathbf{C}}_{\text{li}}^{\text{b}}$ is the DCM from the computed navigation frame of the SINS (p-frame) to the b-frame, i.e., \mathbf{C}_p^{b} . If the attitude errors between the p-frame and the li-frame, $\boldsymbol{\varphi}$, are small enough, there is

$$\hat{\mathbf{C}}_{\text{li}}^{\text{b}} = \mathbf{C}_p^{\text{b}} = \mathbf{C}_{\text{li}}^{\text{b}} \mathbf{C}_p^{\text{li}} = \mathbf{C}_{\text{li}}^{\text{b}} (\mathbf{I} + \boldsymbol{\Phi}) \tag{17}$$

where \mathbf{C}_p^{li} is the DCM from the p-frame to the li-frame and $\boldsymbol{\Phi}$ is the skew-symmetric matrix of $\boldsymbol{\varphi}$. Substituting Equation (17) into Equation (16) yields

$$\hat{\mathbf{I}}_{\text{INS},1,k}^{\text{s}} = \mathbf{C}_b^{\text{s}} \mathbf{C}_{\text{li}}^{\text{b}} (\mathbf{I} + \boldsymbol{\Phi}) \mathbf{I}_{1,k}^{\text{li}} \tag{18}$$

The measurement of the navigation filter at the time k , $\mathbf{z}_{1,k}$, is determined by the difference between the unit vectors estimated by the pre-filter and the SINS

$$\mathbf{z}_{1,k} = \hat{\mathbf{I}}_{\text{CNS},1,k}^{\text{s}} - \hat{\mathbf{I}}_{\text{INS},1,k}^{\text{s}} = \mathbf{v}_{\text{CNS},1,k} - \mathbf{C}_b^{\text{s}} \mathbf{C}_{\text{li}}^{\text{b}} \boldsymbol{\Phi} \mathbf{I}_{1,k}^{\text{li}} \tag{19}$$

Since $\mathbf{C}_{\text{li}}^{\text{b}}$ cannot be output by the SINS, Equation (19) can be modified as

$$\mathbf{z}_{1,k} = \mathbf{v}_{\text{CNS},1,k} - \mathbf{C}_b^{\text{s}} \left(\hat{\mathbf{C}}_{\text{li}}^{\text{b}} - \mathbf{C}_{\text{li}}^{\text{b}} \boldsymbol{\Phi} \right) \boldsymbol{\Phi} \mathbf{I}_{1,k}^{\text{li}} = -\mathbf{C}_b^{\text{s}} \hat{\mathbf{C}}_{\text{li}}^{\text{b}} \boldsymbol{\Phi} \mathbf{I}_{1,k}^{\text{li}} + \mathbf{v}_{1,k} = \mathbf{C}_b^{\text{s}} \hat{\mathbf{C}}_{\text{li}}^{\text{b}} \mathbf{L}_{1,k}^{\text{li}} \boldsymbol{\varphi} + \mathbf{v}_{1,k} \tag{20}$$

where $\mathbf{L}_{1,k}^{\text{li}}$ is the skew symmetric matrix of $\mathbf{I}_{1,k}^{\text{li}}$ and $\mathbf{v}_{1,k} = \mathbf{v}_{\text{CNS},1,k} + \mathbf{C}_b^{\text{s}} \mathbf{C}_{\text{li}}^{\text{b}} \boldsymbol{\Phi}^2 \mathbf{I}_{1,k}^{\text{li}}$. Since it is assumed that the attitude errors $\boldsymbol{\varphi}$ are small enough, the second term of $\mathbf{v}_{1,k}$ can be neglected so there is $\mathbf{v}_{1,k} \approx \mathbf{v}_{\text{CNS},1,k}$. The covariance matrix of $\mathbf{v}_{1,k}$, $\mathbf{R}_{1,k}$ is approximated as the covariance matrix of the steady state error of the pre-filter $\mathbf{P}_{\text{pre},1,k}$, i.e., $\mathbf{R}_{1,k} \approx \mathbf{P}_{\text{pre},1,k}$.

If N stars are pre-filtered, the measurements are written as $\mathbf{z}_k = [\mathbf{z}_{1,k}^{\text{T}} \quad \mathbf{z}_{2,k}^{\text{T}} \quad \dots \quad \mathbf{z}_{N,k}^{\text{T}}]^{\text{T}}$. The measurement equations for the navigation filter are

$$\begin{cases} \mathbf{z}_k = \mathbf{H}_k \mathbf{x}_k + \mathbf{v}_k \\ \mathbf{H}_k = \begin{bmatrix} \mathbf{C}_b^{\text{s}} \hat{\mathbf{C}}_{\text{li}}^{\text{b}} \mathbf{L}_{1,k}^{\text{li}} & \mathbf{0}_{3 \times 3} \\ \mathbf{C}_b^{\text{s}} \hat{\mathbf{C}}_{\text{li}}^{\text{b}} \mathbf{L}_{2,k}^{\text{li}} & \mathbf{0}_{3 \times 3} \\ \vdots & \vdots \\ \mathbf{C}_b^{\text{s}} \hat{\mathbf{C}}_{\text{li}}^{\text{b}} \mathbf{L}_{N,k}^{\text{li}} & \mathbf{0}_{3 \times 3} \end{bmatrix} \\ \mathbf{v}_k = [\mathbf{v}_{1,k}^{\text{T}} \quad \mathbf{v}_{2,k}^{\text{T}} \quad \dots \quad \mathbf{v}_{N,k}^{\text{T}}]^{\text{T}} \end{cases} \tag{21}$$

Since the identified stars are shifting and the number of the identified stars is variable in the filtering, the measurements of the navigation filter are processed sequentially.

As both the state and the measurement equations of the navigation filter are linear, the standard Kalman filter can be applied.

Table 1. The specifications of the star sensor.

FOV	CCD focal plane	Pixel size	Focal length	Exposure	Exposure index	Magnitude threshold	Radius of Gaussian PSF
$15^\circ \times 15^\circ$	512×512	$27 \mu\text{m}$	98.9 mm	100 ms	1	7 Mv	0.67 pixel

5. SIMULATIONS. The simulated star images are based on the Smithsonian Astrophysical Observatory (SAO) star catalogue J2000. Only the stars with the magnitude no greater than 7 Mv are simulated. The energy distribution of the simulated stars is as follows

$$G(x, y) = AG_{\text{norm}}(x, y) \quad (22)$$

where A is the amplitude and $G_{\text{norm}}(x, y)$ as described by Wang et al. (2012) is the normalised energy distribution. The value of A is determined by both the exposure and the magnitude threshold that a star sensor can image. Since the magnitude threshold of the star sensor is set as 7 Mv, the amplitude of a 7 Mv star image is five times the noise Standard Deviation (STD) when there is no vehicle manoeuvring. The amplitude of the star with other magnitudes can be derived as

$$A_2 = 2.512^{M_1 - M_2} \times A_1 \quad (23)$$

where A_1 and A_2 are the amplitudes of the star images with the magnitudes of M_1 and M_2 where $M_1 = 7$ Mv. The specifications of the star sensor are listed in Table 1. CCD and PSF in Table 1 are the abbreviations of Charge Coupled Device and Power Spectral Function respectively. The errors of gyroscope and accelerometer are assumed as first order Markov processes with the time constants τ_{acc} and τ_{gyro} of 1800 s and 7200 s respectively. The exciting noise strengths of the Markov processes for gyroscope and accelerometer are $0.2^\circ/\text{h}$ and 1×10^{-6} g respectively. The output rate of the star sensor is 1 Hz and that of the gyroscope and the accelerometer is 100 Hz.

The simulated trajectory for a ballistic missile starts from a point (112°E , 39°N) on the Earth and lasts for 1500 s. The star sensor does not work for 160 s during the boost and ascent phase. The reentry phase is not included in the trajectory since the star sensor does not work in this phase either. Figure 3 illustrates the Three Dimensional (3D) path and the height of the trajectory. It is assumed that the initial alignment for the SINS has been accomplished before the integration (Wang et al., 2015). The initial values of pitch, yaw and roll errors are $10''$, $30''$, and $10''$, respectively. The proposed integration is compared with the existing integration shown in Figure 1 in the following simulations. The angular separation algorithm is employed both in the existing integration and in the acquisition mode of the proposed integration so that the integrations are effective when there are only two stars identified. The triad algorithm is employed to determine attitude as only two stars are identified in the integrations while the Quaternion Estimator (QUEST) algorithm is employed when more than two stars are identified (Yang, 2012; Harold, 1964; Shuster and Oh, 1981). AD is performed in the navigation filter in the tracking mode of the proposed integration so that the existing AD algorithms are unnecessary.

5.1. *All identified stars with the same centroid extracting error.* Figure 4 depicts the AD results of the integrations when two and three stars are identified with the CE error of 0.05 pixel. Table 2 lists the means and the STDs of the attitude errors in arc seconds

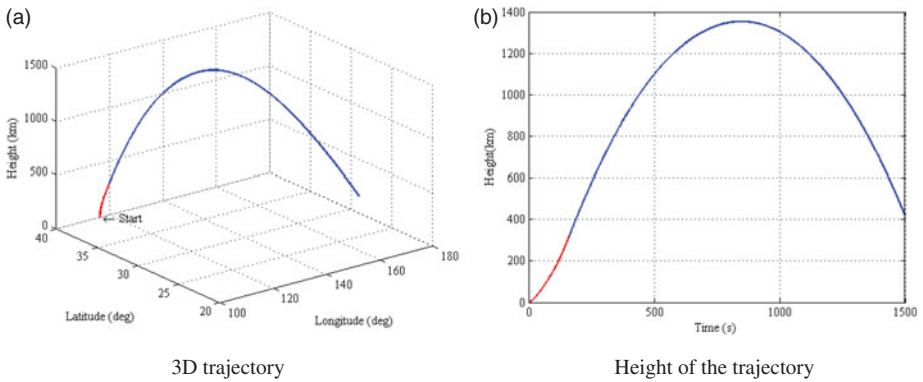


Figure 3. Simulated trajectory for a ballistic missile.

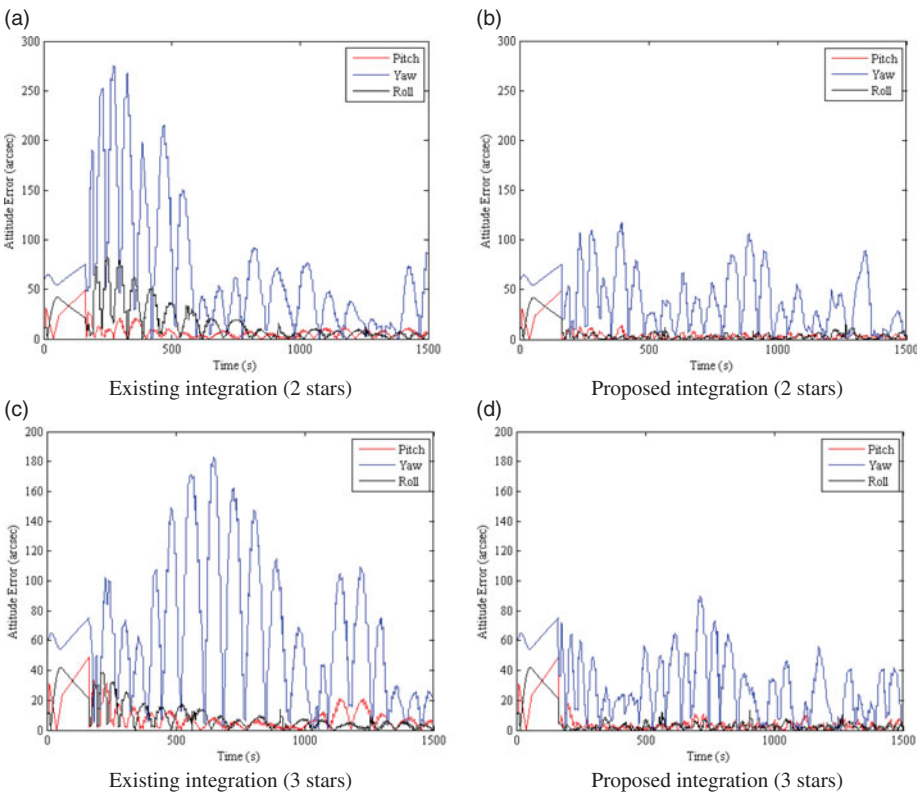


Figure 4. Attitude errors of the integrations with the same CE error (0.05 pixel).

when two to five stars are identified. Since the integrations are run after 160 s, the errors in Table 2 are calculated from 160 s to the end. It is assumed that all the identified stars have the same CE error which is a zero-mean Gaussian white noise with the STD of 0.01, 0.05, and 0.1 pixel respectively.

Table 2. Attitude errors of the integrations.

CE error	Number of stars		2		3		4		5	
			Mean	STD	Mean	STD	Mean	STD	Mean	STD
0.01	Existing integration	Pitch	1.08	6.76	1.07	6.38	1.00	6.31	1.00	6.22
		Yaw	0.75	15.81	2.57	12.08	1.01	10.87	1.78	10.06
		Roll	0.90	8.05	0.91	6.20	0.90	5.93	0.75	4.54
	Proposed integration	Pitch	1.49	3.43	1.51	3.34	1.48	3.31	1.46	3.28
		Yaw	1.90	15.65	1.57	10.09	1.42	8.71	0.95	7.79
		Roll	0.43	2.46	0.38	2.28	0.42	2.24	0.42	2.26
0.05	Existing integration	Pitch	1.03	9.97	0.02	7.99	0.56	7.85	0.80	5.91
		Yaw	0.14	92.69	1.03	79.01	6.08	63.84	2.91	42.58
		Roll	1.63	23.81	0.55	13.86	1.70	11.40	0.35	10.57
	Proposed integration	Pitch	1.20	5.03	1.26	4.97	1.31	4.56	1.90	4.10
		Yaw	1.52	48.08	2.45	34.11	5.00	27.57	0.19	25.01
		Roll	0.61	4.05	0.63	3.74	0.45	3.36	0.78	2.99
0.10	Existing integration	Pitch	0.98	18.38	2.04	12.40	1.22	11.24	1.00	10.38
		Yaw	24.13	180.05	8.86	129.64	5.41	101.82	12.07	74.26
		Roll	1.49	21.13	0.39	19.86	0.34	16.26	0.46	14.17
	Proposed integration	Pitch	0.97	10.16	1.92	7.72	1.44	6.48	1.46	5.79
		Yaw	1.04	117.65	3.79	72.31	3.18	52.34	1.07	51.52
		Roll	0.79	11.14	0.07	6.37	0.13	5.84	0.17	5.06

According to the results, the proposed integration has a smaller attitude error than the existing integration. The yaw error of the proposed integration is close to that of the existing integration when only two stars are identified. In fact, the yaw error is significantly larger than the other two angular errors in both integrations. The reason is that the yaw is corresponding to the angle around the optical axis of the star sensor while the AD accuracy around the optical axis of the star sensor is significantly lower than those across the optical axis (Wu and Wang, 2011).

Compared with the existing integration, the yaw error is reduced significantly in the proposed integration when there are more than two identified stars. The point where the performance of the proposed integration outperforms that of the existing integration lies in the pre-filters in the proposed integration. Although the CE errors of all identified stars are the same in distribution in the simulations, the CE error of one star may be very different from that of another since the CE error is a Gaussian white noise. In the proposed integration, the errors of the starlight directions are estimated by the pre-filters and the navigation filter allocates the corresponding weights to the starlight directions according to Equation (20). However, all the identified stars have the same weights to determine attitude in the existing integration so that the attitude accuracy is significantly influenced by the stars with lower accuracy. Therefore, the proposed integration can provide more accurate and stable attitude than the existing integration.

According to Table 2, with the decrease of the CE error of the identified stars, the attitude accuracy of the two integrations is improved significantly. With the increase of the number of the identified stars, the attitude accuracy of the two integrations tends to improve while the attitude error of the proposed integration is not reduced significantly when there are more than two identified stars. Hence the identified stars are no more than three in the following simulations.

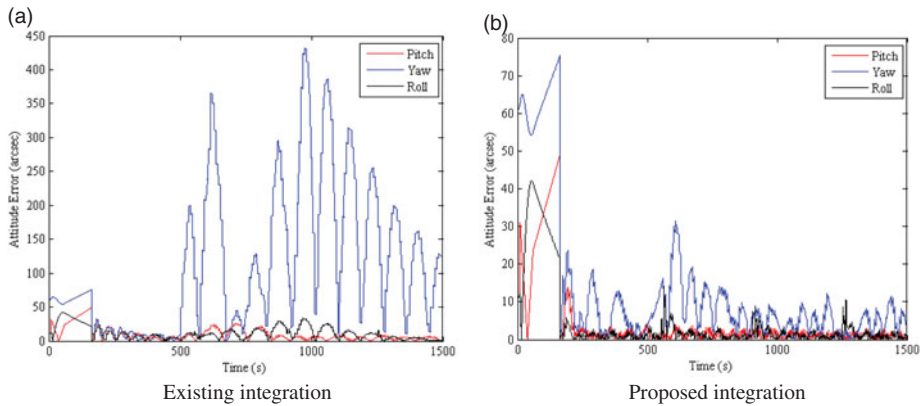


Figure 5. Attitude errors of the integrations with three identified stars and one star having 0.5 pixel CE error.

Table 3. Attitude errors of the integrations with one low accuracy star.

CE error	Number of stars		2		3	
			Mean	STD	Mean	STD
0-01, 0-10	Existing integration	Pitch	1.52	8.16	0.54	7.17
		Yaw	10.34	54.78	1.41	20.29
		Roll	1.07	6.88	0.58	6.85
	Proposed integration	Pitch	1.66	3.96	1.49	3.35
		Yaw	6.30	39.17	0.36	9.02
		Roll	1.10	4.82	0.38	2.45
0-01, 0-20	Existing integration	Pitch	0.55	11.23	1.44	7.20
		Yaw	16.50	133.09	11.46	60.02
		Roll	1.12	8.90	0.45	7.45
	Proposed integration	Pitch	0.75	7.29	1.46	3.32
		Yaw	10.92	114.80	0.92	10.00
		Roll	0.94	10.69	0.43	2.25
0-01, 0-50	Existing integration	Pitch	4.43	31.51	1.15	10.22
		Yaw	20.21	236.95	9.79	163.55
		Roll	2.14	26.67	0.99	12.01
	Proposed integration	Pitch	1.25	9.80	1.54	3.35
		Yaw	4.71	228.70	1.39	15.36
		Roll	0.13	13.71	0.48	2.28

5.2. *AD with one large error star.* Figure 5 shows the AD results of the integrations when three stars are identified. Table 3 lists the means and the STDs of the attitude errors in arc seconds when two and three stars are identified. It is also assumed that all the identified stars have the same CE error, a zero-mean Gaussian white noise with the STD of 0.01 pixels, except that the STD of one star's CE error is 0.1, 0.2 and 0.5 pixels respectively from 500 s to 1000 s. According to the results, the attitude errors of the existing integration will increase significantly when one star's CE error increases sharply no matter whether two or three stars are identified. The attitude errors of the proposed integration will also increase significantly with the degradation of one star's CE when only two stars are identified, but they are very small if there are three identified stars. Hence, the proposed integration is more reliable than the existing integration when more than two stars are identified.

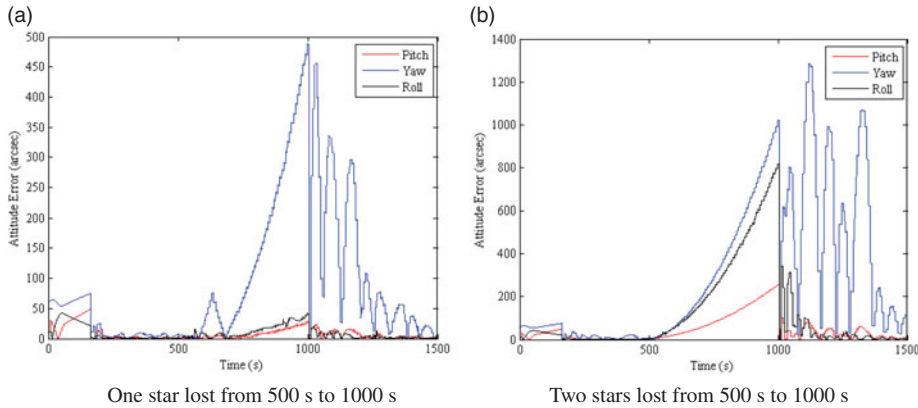


Figure 6. Attitude errors of the proposed integration with two identified stars.

5.3. *Only one identified star.* Figure 6 depicts the attitude errors of the proposed integration when only two stars are identified and one or two stars are lost from 500 s to 1000 s. Since the existing integration will run in the single SINS mode if only one star is identified, only the proposed integration is investigated in this simulation. If two stars are identified, the results of the proposed integration are the same as the above results. However, if only one star is identified from 500 s to 1000 s, the attitude errors will increase severely; if no star is identified from 500 s to 1000 s, the integration will run in the single SINS mode and the attitude errors will diverge in the SINS mode. The attitude errors of the proposed integration with only one identified star diverge too, but they are effectively compensated in the interval of (500 s, 580 s). Hence, the proposed integration is still effective if only one star is identified for a limited time span.

6. CONCLUSIONS. To improve the reliability of the integration of the SINS with the star sensor, a new integration, composed of pre-filters and a cascaded navigation filter, is proposed. A pre-filter is designed for each identified star. The starlight direction of an identified star and its error are estimated by the pre-filter so that the cascaded navigation filter can acquire the optimal estimation. The simulation results prove that the proposed integration is more accurate and reliable than the existing integration. The proposed integration can work effectively for a worthwhile period even when only one star is identified.

REFERENCES

- Ali, J. and Fang, J. C. (2006). SINS/ANS integration for augmented performance navigation solution using unscented Kalman filtering. *Aerospace Science and Technology*, **10**(3), 233–238.
- Bar-Itzhach, I. Y., Serfaty, D. and Vitek, Y. (1982). Doppler-aided low-accuracy strapdown inertial navigation system. *Journal of Guidance, Control, and Dynamics*, **5**(3), 236–242.
- Batista, P., Silvestre, C. and Oliveira, P. (2011). Vector-based attitude filter for space navigation. *Journal of Intelligent and Robotic Systems: Theory and Applications*, **64**(2), 221–243.
- Hablani, H. B. (2009). Autonomous inertial relative navigation with sight-line-stabilized integrated sensors for spacecraft rendezvous. *Journal of Guidance, Control and Dynamics*, **32**(1), 172–183.
- Harold, D. B. (1964). A passive system for determining the attitude of a satellite. *AIAA Journal*, **2**(7), 1350–1351.
- He, Z., Wang, X. and Fang, J. (2014). An innovative high-precision SINS/CNS deep integrated navigation scheme for the Mars rover. *Aerospace Science and Technology*, **39**, 559–566.

- Ho, K. (2012). A survey of algorithms for star identification with low-cost star trackers. *Acta Astronautica*, **73**, 156–163.
- Huffman, K. M. (2006). *Designing star trackers to meet micro-satellite requirements*. Massachusetts Institutes of Technology.
- Johnson, W. M. and Phillips, R. E. (2001). Steller/inertial (EBCCD/MEMS) attitude measurement & control of small satellites. *Proceedings of AIAA Space Conference and Exposition, Albuquerque, NM, USA*, August 28–30.
- Ju, G. and Junkins, J. L. (2003). Overview of star tracker technology and its trends in research and development. *Advances in the Astronautical Sciences*, **115**, 461–477.
- Lashley, M., Bevil, D. M. and Hung, J. Y. (2009). Performance analysis of vector tracking algorithms for weak GPS signals in high dynamics. *IEEE Journal on Selected Topics in Signal Processing*, **3**(4), 661–673.
- Levine, S., Dennis, R. and Bachman, K. L. (1990). Strapdown Astro-inertial navigation utilizing the optical wide-angle lens startracker. *Navigation: Journal of the Institute of Navigation*, **37**(4), 347–362.
- Liebe, C. C. (1995). Star trackers for attitude determination. *IEEE Aerospace and Electronic Systems Magazine*, **10**(6), 10–16.
- Liebe, C. C. (2002). Accuracy Performance of Star Trackers: A Tutorial. *IEEE Transactions on Aerospace and Electronic Systems*, **38**(2), 587–599.
- Liu, B., Wang, K. and Zhang, C. (2011). Star pattern recognition algorithm aided by inertial information. *Proceedings of SPIE, 8196, Beijing, China*.
- Ning, X., Gui, M., Xu, Y., Bai, X. and Fang, J. (2016). INS/VNS/CNS integrated navigation method for planetary rovers. *Aerospace Science and Technology*, **48**, 102–114.
- Percival, J. W., Nordsieck, K. H. and Jaehnig, K. P. (2008). The ST5000: a high-precision star tracker and attitude determination system. *Proceedings of SPIE, 7010, 70104H-1–70104H-6*.
- Rad, A. M., Nobari, J. H. and Nikkhah, A. A. (2014). Optimal attitude and position determination by integration of INS, star tracker, and horizon sensor. *IEEE Aerospace and Electronic Systems Magazine*, **29**(4), 20–33.
- Scholl, M. S. (1995). Star-field identification for autonomous attitude determination. *Journal of Guidance, Control and Dynamics*, **18**(1), 61–65.
- Shuster, M. D. and Oh, S. D. (1981). Three-axis attitude determination from vector observations. *Journal of Guidance and Control*, **4**(1), 70–77.
- Silani, E. and Lovera, M. (2006). Star identification algorithm: novel approach & comparison study. *IEEE Transactions on Aerospace and Electronic Systems*, **42**(4), 1275–1288.
- Sun, T., Xing, F., You, Z. and Li, B. (2014). Deep coupling of star tracker and MEMS-gyro data under highly dynamic and long exposure conditions. *Measurement Science and Technology*, **25**(8), 1–15.
- Wang, H., Zhou, W. and Cheng, X. (2012). Image smearing modeling and verification for strap-down star sensor. *Chinese Journal of Aeronautics*, **25**(1), 115–123.
- Wang, K., Zhang, C. and Yong, L. (2014). A new restoration algorithm for the smeared image of a SINS-aided star sensor. *Journal of Navigation*, **67**, 881–898.
- Wang, X., Guan, X., Fang, J. and Li, H. (2015). A high accuracy multiplex two-position alignment method based on SINS with the aid of star sensor. *Aerospace Science and Technology*, **42**, 66–73.
- Wu, X., and Wang, X. (2011). A SINS/CNS deep integrated navigation method based on mathematical horizon reference. *Aircraft Engineering and Aerospace Technology*, **83**(1), 26–34.
- Wu, X., and Wang, X. (2011). Multiple blur of star image and the restoration under dynamic conditions. *Acta Astronautica*, **68**(11-12), 1903–1913.
- Xu, F. and Fang, J. (2008). Velocity and position error compensation using strapdown inertial navigation system/celestial navigation system integration based on ensemble neural network. *Aerospace Science and Technology*, **12**(4), 302–307.
- Yang, Y. (2012). Spacecraft attitude determination and control: quaternion based method. *Annual Reviews in Control*, **36**, 198–219.